Intracellular fate of LDL receptor family members depends on the cooperation between their ligand-binding and EGF domains

Dennis Van Hoof, Kees W. Rodenburg* and Dick J. Van der Horst

Department of Biochemical Physiology and Institute of Biomembranes, Utrecht University, Padualaan 8, 3584 CH Utrecht, The Netherlands

*Author for correspondence (e-mail: k.w.rodenburg@bio.uu.nl)

Accepted 13 January 2005
Journal of Cell Science 118, 1309-1320 Published by The Company of Biologists 2005
doi:10.1242/jcs.01725

Summary

The insect low-density lipoprotein (LDL) receptor (LDLR) homologue LpR mediates endocytosis of an insect lipoprotein (lipophorin) that is structurally related to LDL. Despite these similarities, lipophorin and LDL follow distinct intracellular routes upon endocytosis by their receptors. Whereas LDL is degraded in lysosomes, lipophorin is recycled in a transferrin-like manner. We constructed several hybrid receptors composed of *Locusta migratoria* LpR and human LDLR regions to identify the domains implicated in LpR-mediated ligand recycling. Additionally, the triadic His562 residue of LDLR, which is putatively involved in ligand uncoupling, was mutated to Asn, corresponding to Asn643 in LpR, to analyse the role of the His triad in receptor functioning. The familial hypercholesterolaemia (FH) class 5 mutants $LDLR_{H562Y}$ and $LDLR_{H190Y}$ were also analysed in vitro. Fluorescence microscopic investigation and quantification suggest that LpR-mediated ligand recycling involves cooperation between the ligand-binding domain and epidermal growth factor (EGF) domain of LpR, whereas its cytosolic tail does not harbour motifs that affect this process. LDLR residue His562 appears to be essential for LDLR recycling after ligand endocytosis but not for constitutive receptor recycling. Like $LDLR_{H562N}$, $LDLR_{H562Y}$ did not recycle bound ligand; moreover, the intracellular distribution of both mutant receptors after ligand incubation coincides with that of a lysosomal marker. The LDLR mutant characterization in vitro suggests that LDLR FH class 5 mutations might be divided into two subclasses.

Key words: Lipophorin, Lipoprotein, Transferrin, Receptor, Endocytosis, Recycling

Introduction

The insect homologue of the mammalian low-density lipoprotein (LDL) receptor (LDLR) family binds the insect lipoprotein lipophorin (Lp) and mediates Lp endocytosis (Dantuma et al., 1999; Van Hoof et al., 2002). The receptor (LpR) is expressed by the insect fat body and is assumed to be involved in the storage of lipids derived from circulating Lp (Van Hoof et al., 2003). The protein component of Lp is structurally related to that of LDL (Babin et al., 1999; Mann et al., 1999; Segrest et al., 2001). Moreover, LpR is highly homologous to mammalian LDLR and has an identical domain composition (Dantuma et al., 1999). Yet, the intracellular route of Lp is remarkably different from that of LDL (Van Hoof et al., 2002; Van Hoof et al., 2005).

For LDL, in vitro experiments showed that, upon endocytosis by LDLR, bound lipoprotein is uncoupled from the receptor in tubulo-vesicular sorting endosomes owing to mild acidification of the vesicle lumen (Mukherjee et al., 1997). The receptors accumulate in the tubules that bud off to be transported back to the plasma membrane via the endocytic recycling compartment (ERC) (Maxfield and McGraw, 2004), whereas the sorting endosomes mature into lysosomes (Stoorvogel et al., 1991), wherein the luminal constituents (i.e. released ligands) are degraded (Goldstein et al., 1985; Brown and Goldstein, 1986). In contrast to the lysosomal fate of LDL, LpR-mediated uptake of Lp eventually appeared to result in ligand recycling (Van Hoof et al., 2002; Van Hoof et al., 2005). Lp is proposed to remain attached to LpR in sorting endosomes and to escape from lysosomal hydrolysis. Similar to LDLR, LpR is recycled back to the plasma membrane via the ERC (Van Hoof et al., 2002). Consequently, analogous to transferrin (Tf) after endocytosis by the Tf receptor (TfR) (Yamashiro et al., 1984; McGraw et al., 1987), Lp is resecreted.

The distinct intracellular routes of Lp and LDL suggest that specific structural differences between the two receptors effect a dissimilar ligand distribution. Elucidation of the X-ray crystal structure of the LDLR ectodomain at endosomal pH revealed that LDLR adopts an arched conformation in which the ligand-binding domain is folded onto the β-propeller of the epidermal growth factor (EGF) precursor homology domain (Rudenko et al., 2002). A pH-dependent conformational change provoked by acidification of the vesicle lumen is assumed to result in the displacement of LDL from the ligand-binding domain (Innerarity, 2002; Jeon and Blacklow, 2003). Three His residues (His190 in the ligand-binding domain and His562 and His586 in the EGF domain), which become protonated below pH 6.7, reside in the interface of the fold. His562 and His586 are proposed to be important for ligand dissociation (Jeon and Blacklow, 2003). Tertiary structural analysis revealed that one

triadic His residue is not present in LpR; at the position corresponding to His562 in LDLR, LpR contains Asn643 instead (Fig. 1).

Mutations in the LDLR-encoding gene that affect crucial steps in the LDL uptake mechanism result in familial hypercholesterolaemia (FH). These mutations have been classified according to the stage at which LDLR functioning is disturbed (Hobbs et al., 1992). Normally, LDLR is internalized and recycled either with or without antecedent ligand binding, and has a life span of ~150 endocytic cycles (Goldstein et al., 1979). FH class-5 mutations affect receptor recycling and are predominantly mapped to the EGF domain (Hobbs et al., 1992). Whereas FH mutations of His586 have not yet been described, mutation of His562 to Tyr has been found in independent families clinically diagnosed with FH (Sun et al., 1994) (J. C. Defesche, personal communication). The latter mutation is assumed to impair ligand dissociation and subsequent receptor recycling, resulting in the degradation of the receptor (i.e. class 5). However, the intracellular fates of FH class-5 mutant receptors, such as $LDLR_{H562Y}$, have not been analysed at the cellular level. Notably, even though a triadic His residue is also absent at the corresponding position in wild-type (wt) LpR, this insect receptor is able to recycle without, as well as in complex with, ligand (Van Hoof et al., 2002).

In the present study, hybrid receptors composed of domains of *Locusta migratoria* LpR and human LDLR were constructed to determine which LpR domains contain unique motifs that are essential for recycling of the receptor-ligand complex after endocytosis. In addition, to investigate the role of the His triad in receptor recycling, the triadic His562 residue of LDLR was mutated to Asn ($LDLR_{H562N}$), corresponding to Asn643 in LpR. Likewise, we mutated LDLR His562 to Tyr ($LDLR_{H562Y}$) and LDLR His190 to Tyr ($LDLR_{H190Y}$) to analyse the naturally occurring FH mutations in vitro. The results suggest that the ligand-binding domain and EGF domain cooperate during LpR-driven ligand recycling, whereas the intracellular tail has no significant role in this process. The His562 residue in LDLR is essential for recycling of the receptor in the presence of lipoprotein, whereas receptor recycling was not altered in the absence of the ligand. From the endocytic capability and intracellular pathway of these mutants, we additionally propose that LDLR FH class 5 mutations might be divided into two subclasses.

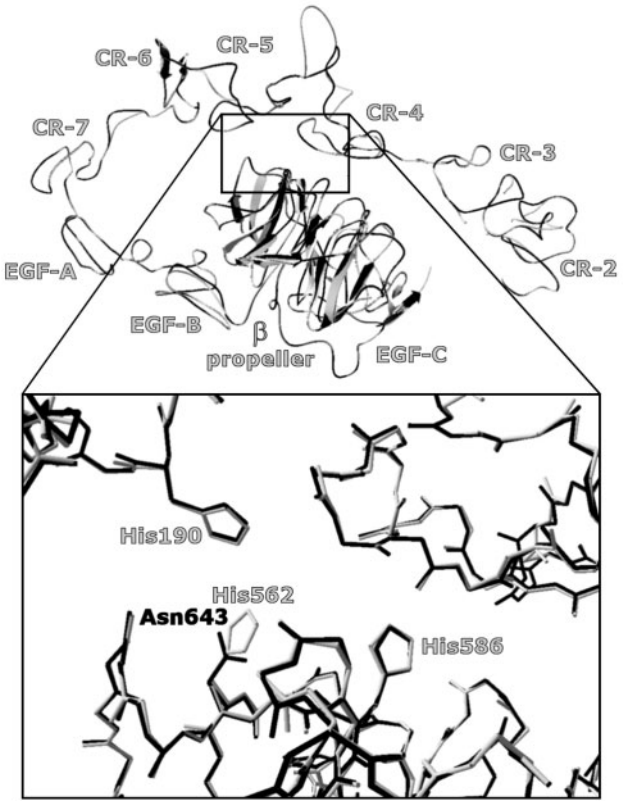

Fig. 1. Construction of a three-dimensional model of the structure of the LpR ectodomain from the third cysteine-rich repeat to the EGF-C module (black). The LpR structure is superimposed onto the X-ray crystal structure of the LDLR ectodomain from the second cysteine-rich repeat to the EGF-C module at pH 5.3 (grey); this reveals that His562 in LDLR corresponds to Asn643 in LpR. Enlargement of the frame shows the side chains of His190, His562 and His586 of LDLR (grey) in the interface between cysteine-rich repeats 4 and 5 of the ligand-binding domain and the β-propeller of the EGF domain in LDLR, and the Asn643 residue in LpR (black). CR, cysteine-rich repeats.

Materials and Methods

Three-dimensional modelling of the LpR ectodomain

The on-line program Swiss-Model (http://swissmodel.expasy.org/) was used to generate a three-dimensional reconstruction of the LpR ectodomain (Guex and Peitsch, 1997; Schwede et al., 2003). Alignments with LpR domains were made of the regions from Gln128 to Cys205 and Pro206 to Ala773 with PDB entry 1N7D (http://www.rcsb.org/pdb/) as template using the First Approach mode. These alignments were manually optimized to 77% sequence similarity and used as input data for construction of a three-dimensional model based on the elucidated crystal structure of the LDLR ectodomain at pH 5.3 (Rudenko et al., 2002). The modelled LpR domains were superimposed onto the structure of LDLR using Swiss PDB Viewer 3.6b3.

Antibodies, reagents and proteins

LysoTracker (LT) L-7528 (Molecular Probes) was kindly provided by A. E. M. Klomp (Department of Metabolic and Endocrine Diseases, University Medical Center, Utrecht, The Netherlands) and FITC-labelled goat anti-mouse antibody (FITC-GAM) (Jackson ImmunoResearch Laboratories) was a generous gift from I. Sorokina (Department of Molecular Cell Biology, Utrecht University, Utrecht, The Netherlands). Zeocin (Invivogen), TRITC-labelled goat anti-mouse antibody (TRITC-GAM) (Jackson ImmunoResearch Laboratories) and restriction enzymes (New England BioLabs) were obtained from commercial sources. Details on all other materials have been described (Van Hoof et al., 2002; Van Hoof et al., 2003; Van Hoof et al., 2005).

Cell culture

CHO cells were cultured in 25 cm^2 polystyrene culture flasks (CellStar) as described (Van Hoof et al., 2002). Growth medium for cells transfected with pcDNA3 or pcDNA3.1/Zeo(+) plasmid was supplemented with 400 μg ml^{-1} G-418 or 400 μg ml^{-1} Zeocin, respectively. In addition, 0.2 μM mevalonate was added to growth medium of *ldlA*(LDLRΔEGF) transfectants (Davis et al., 1987), a generous gift from J. L. Goldstein (Department of Molecular

Genetics, University of Texas Southwestern Medical Center at Dallas, TX, USA).

Construction of mammalian expression vectors harbouring lipoprotein receptor cDNA constructs

pcDNA3-LDLR was constructed by subcloning the LDLR cDNA from pBS-LDLR (a generous gift from L. J. Braakman, Department of Bio-Organic Chemistry, Utrecht University, Utrecht, The Netherlands) to pcDNA3.1/Zeo(+) (Invitrogen) using the restriction enzymes *Kpn*I and *Not*I.

pcDNA3-LpR$_{1\text{-}790}$LDLR$_{791\text{-}839}$ was made from PCR fragments amplified with SuperTaq DNA polymerase (Sphaero-Q) and synthetic oligonucleotides (Invitrogen). The LpR region from Val683 to Arg797 was amplified by PCR using primers 5′-CACGTGTATCATC-CATATCGACAACC-3′ (underlining indicates an introduced *Eco*72I site) and 5′-CTCGAGTCTTAAGCCGCCAGTTGTAAACTACCA-GAGCCACTATAGC-3′ (underlining indicates an introduced *Afl*II and *Xho*I site), and the piLR-e plasmid (Dantuma et al., 1999) as template DNA. The PCR fragment was ligated into pGEM-T (Promega), generating pGEM-T-LpR$_{683\text{-}797}$. Similarly, the untranslated region (UTR) from the stop codon to the *Cla*I site was amplified using primers 5′-CTCGAGGTTAGTTCAGTAACTGAC-3′ (underlining indicates an introduced *Xho*I site) and 5′-ATCGATTATGATTATA-TTTTGTACTTAATAACC-3′ (underlining indicates an introduced *Cla*I site), and piLR-e as template DNA. The PCR fragment was ligated into pGEM-T, generating pGEM-T-LpR$_{STOP\text{-}ClaI}$. The PCR fragment in pGEM-T-LpR$_{STOP\text{-}ClaI}$ was subcloned into pGEM-T-LpR$_{683\text{-}797}$ after digestion with *Xho*I and *Not*I; the latter restriction site resides in the multiple cloning site of pGEM-T. The fragment separating the two LpR regions was substituted after digestion with *Afl*II and *Xho*I by annealed synthetic oligonucleotides encoding LDLR$_{791\text{-}STOP}$ flanked by *Afl*II and *Xho*I sticky ends. The final product was ligated into piLR-e after digestion with *Eco*72I and *Cla*I, generating pcDNA3-LpR$_{1\text{-}790}$LDLR$_{791\text{-}839}$.

pcDNA3-LpR$_{1\text{-}342}$LDLR$_{293\text{-}839}$ and pcDNA3-LDLR$_{1\text{-}292}$LpR$_{343\text{-}850}$ were constructed from PCR fragments. LpR$_{1\text{-}342}$ was amplified with primers 5′-GAATTCGGCTTCACGGGAGG-3′ (underlining indicates an introduced *Eco*RI site) and 5′-CATTCATTGGTACCA-CATTTTTCTTGTGG-3′ (underlining indicates an introduced *Kpn*I site), and piLR-e as template DNA. LDLR$_{293\text{-}839}$ was amplified with primers 5′-GCGGTACCAACGAATGCTTGG-3′ (underlining indicates an introduced *Kpn*I site) and 5′-ATTTAAATTCACGC-CACGTCATCCTCC-3′ (underlining indicates an introduced *Swa*I site), and pBS-LDLR as template DNA. LDLR$_{1\text{-}292}$ was amplified with primers 5′-AAGCTTCTGGCAGAGGCTGCGAGC-3′ (underlining indicates an introduced *Hin*dIII site) and 5′-GGTACCG-CACTCTTTGATGGG-3′ (underlining indicates an introduced *Kpn*I site), and the plasmid pBS-LDLR as template DNA. LpR$_{343\text{-}850}$ was amplified with primers 5′-GGTACCAATGAATGTGCTG-TAAATAATGG-3′ (underlining indicates an introduced *Kpn*I site) and 5′-GCGGCCGCTTATACATAATCATTTGTCCC-3′ (underlining indicates an introduced *Not*I site), and piLR-e as template DNA. All the PCR fragments were ligated into pGEM-T. The PCR fragment in pGEM-T-LpR$_{1\text{-}342}$ was subcloned into pGEM-T-LDLR$_{293\text{-}839}$ after digestion with *Kpn*I and *Sac*II; the latter restriction site resides in the multiple cloning site of pGEM-T. The resulting intermediary construct (pGEM-T-LpR$_{1\text{-}342}$LDLR$_{293\text{-}839}$) was ligated into piLR-e after digestion with *Eco*RI and *Swa*I, generating pcDNA3-LpR$_{1\text{-}342}$LDLR$_{293\text{-}839}$. Similarly, the PCR fragment in pGEM-T-LpR$_{343\text{-}850}$ was subcloned into pGEM-T-LDLR$_{1\text{-}292}$ after digestion with *Kpn*I and *Not*I; the latter restriction site resides in the multiple cloning site of pGEM-T. The resulting intermediary construct (pGEM-T-LDLR$_{1\text{-}292}$LpR$_{343\text{-}850}$) was ligated into pcDNA3.1/Zeo(+) after digestion with *Kpn*I and *Not*I, generating pcDNA3-LDLR$_{1\text{-}292}$LpR$_{343\text{-}850}$.

pcDNA3 vectors harbouring LDLR$_{H190Y}$, LDLR$_{H562Y}$ or LDLR$_{H562N}$ were generated with QuickChange PCR using PfuTurbo DNA polymerase (Stratagene) according to manufacturer's protocol. The DNA mutations (underlined) were introduced using primers 5′-GGCGAGTGCATCTACTCCAGCTGGCGC-3′ (H190Y), 5′-GG-GTTGACTCCAAACTTTACTCCATCTCAAGCATCG-3′ (H562Y) and 5′-GGGTTGACTCCAAACTTAACTCCATCTCAAGCATCG-3′ (H562N), in combination with complementary primers and pBS-LDLR as template DNA. The constructs were subcloned into pcDNA3.1/Zeo(+) (Invitrogen) using the *Kpn*I and *Not*I restriction enzymes.

Transfection of CHO cells with the pcDNA3 constructs

Wild-type CHO cells and CHO cells that do not express functional LDLR (*ldlA*) (Kingsley and Krieger, 1984) were grown to ~90% confluence in 12-wells multidishes (Costar). Wild-type CHO cells were transfected with pcDNA3-LpR$_{1\text{-}790}$LDLR$_{791\text{-}839}$, and *ldlA* cells with pcDNA3-LDLR, pcDNA3-LpR$_{1\text{-}342}$LDLR$_{293\text{-}839}$, pcDNA3-LDLR$_{1\text{-}292}$LpR$_{343\text{-}850}$, pcDNA3-LDLR$_{H190Y}$, pcDNA3-LDLR$_{H562Y}$ or pcDNA3-LDLR$_{H562N}$. Transfections were conducted with 3 μg DNA and 5 μl Lipofectamine2000 reagent (Invitrogen Life Technologies) according to the supplier's protocol. Transfected cells were transferred to 75 cm^2 culture flasks (CellStar) and grown for 10 days in growth medium containing 400 μg ml^{-1} G-418 or 400 μg ml^{-1} Zeocin, to obtain transfectants stably expressing the receptors.

Western-blot analysis of cell-membrane extracts

CHO cells were harvested from 25 cm^2 culture flasks at ~90% confluence, after which membrane proteins were isolated, and subjected to SDS-PAGE and western blotting as described (Van Hoof et al., 2002). The blots were incubated with anti-LpR rabbit antibody 2189/90 (1:200), anti-LDLR rabbit antibody 121 (1:2000) or anti--LpR rabbit antibody 9218 (1:200).

Incubation of cells with fluorescently labelled ligands

LDL and Lp were covalently labelled with Oregon Green 488 (OG; Molecular Probes) as described (Van Hoof et al., 2005). Cells were cultured and incubated with 35 μg ml^{-1} OG-labelled LDL (OG-LDL), 25 μg ml^{-1} OG-labelled Lp (OG-Lp) or 25 μg ml^{-1} OG-labelled Tf (OG-Tf) (Molecular Probes), and either immediately fixed in 4% paraformaldehyde or first chased in growth medium at 37°C as described (Van Hoof et al., 2002). When indicated, 25 nM LT was added to the medium 30 minutes before fixation.

Immunofluorescence

Expression of receptors was visualized by immunofluorescence (IF) as described (Van Hoof et al., 2005). TRITC-labelled antibody was used in combination with OG-labelled ligand, and FITC-labelled antibody in combination with LT.

Fluorescence microscopy and image processing

Fixed cells were examined and imaged as described (Van Hoof et al., 2005). Quantification of receptor recycling efficiency (RRE) was conducted by incubating the cells with OG-labelled lipoprotein as indicated, after which the receptor was visualized by IF. The number of cells in which the receptors had perceptibly converged in the ERC was divided by the total number of cells that were capable of internalizing OG-labelled lipoprotein, as indicated in the results section. The *ldlA*(LDLRΔEGF) cell line is monoclonal (Davis et al., 1987), as confirmed by IF using anti-LDLR antibody C7 (i.e. each cell stained positive for the antibody; data not shown). Thus, quantification of *ldlA*(LDLRΔEGF) transfectants that functionally express the receptor (e.g. by ligand incubation) was not needed. Each

data set was the result of a duplicate experiment, except for *ldlA*(LDLRΔEGF) transfectants.

Results

Expression of $LpR_{1-790}LDLR_{791-839}$, $LpR_{1-342}LDLR_{293-839}$ and $LDLR_{1-292}LpR_{343-850}$ by transfected CHO cells

Hybrid receptors composed of *L. migratoria* LpR and human LDLR domains were constructed (Fig. 2) to determine which LpR domains contain unique motifs that are essential for recycling of the receptor-ligand complex after endocytosis. First, the C-terminal cytoplasmic tail of LpR was replaced with that of human LDLR ($LpR_{1-790}LDLR_{791-839}$) to investigate whether this domain of LpR directs intracellular trafficking (i.e. recycling) through interaction with specific cytosolic proteins. To determine the role of the LpR EGF domain in the recycling process, a second hybrid receptor was constructed harbouring the ligand-binding domain of LpR and the region from EGF domain to C-terminus of LDLR ($LpR_{1-342}LDLR_{293-839}$). A reciprocal construct of the latter hybrid receptor, consisting of the ligand-binding domain of LDLR and the rest of LpR ($LDLR_{1-292}LpR_{343-850}$), was made to analyse the involvement of the LpR ligand-binding domain in ligand recycling.

Wild-type CHO cells were stably transfected with the mammalian pcDNA3 expression vector harbouring the $LpR_{1-790}LDLR_{791-839}$ construct, generating polyclonal CHO($LpR_{1-790}LDLR_{791-839}$) cells. Similarly, CHO cells that do not endogenously express LDLR (*ldlA* cells) (Kingsley and Krieger, 1984) were transfected with the other hybrid constructs, producing *ldlA*($LpR_{1-342}LDLR_{293-839}$) and *ldlA*($LDLR_{1-292}LpR_{343-850}$) cell lines. Expression of the hybrid proteins was analysed by western blotting. $LpR_{1-790}LDLR_{791-839}$ and $LpR_{1-342}LDLR_{293-839}$ were detected with anti-LpR antibody 2189/90 (Van Hoof et al., 2003; Van Hoof et al., 2005) raised against the very N-terminal region of the LpR ligand-binding domain. The western blots show that, in addition to wt *L. migratoria* LpR produced by CHO cells transfected with LpR [CHO(LpR) cells], the antibody specifically recognizes both hybrid receptors (Fig. 3A,B). Under reducing conditions, the M_r of LpR (Van Hoof et al., 2002) as well as $LpR_{1-790}LDLR_{791-839}$ is ~150 kDa, whereas that of $LpR_{1-342}LDLR_{293-839}$ is ~160 kDa (Fig. 3A). The difference in M_r between $LpR_{1-342}LDLR_{293-839}$ and the other two receptors coincides with the presence of the LDLR *O*-linked-glycosylation domain, which is probably glycosylated more heavily than that of LpR (Davis et al., 1986). The electrophoretic mobility under reducing conditions (Fig. 3A) is lower than under non-reducing conditions (Fig. 3B), which is consistent with the presence of multiple disulfide bonds in the ligand-binding and EGF domains. The receptors behave similarly under reducing and non-reducing conditions, suggesting that all receptors are folded correctly.

Two antibodies were used to visualize the expression of $LDLR_{1-292}LpR_{343-850}$ (Fig. 2): anti-LpR antibody 9218, which specifically recognizes the very C-terminal amino acids of LpR (Van Hoof et al., 2002; Van Hoof et al., 2003); and anti-LDLR antibody 121, raised against amino acids 59-343 of human LDLR (Jansens et al., 2002). In addition to human LDLR expressed by transfected *ldlA* cells [*ldlA*(LDLR) cells] and endogenous hamster LDLR expressed by wt CHO cells, the anti-LDLR antibody 121 also recognizes immature folding intermediates of non-functional LDLR produced by *ldlA* cells (Fig. 3C) (Van Hoof et al., 2002). Under non-reducing conditions, the hybrid protein is detected by anti-LDLR-121 antibody as well as anti-LpR antibody 9218 (Fig. 3C). $LDLR_{1-292}LpR_{343-850}$ has an electrophoretic mobility identical to wt LpR (Fig. 3C), which can be explained by their mutual glycosylation domain.

Endocytosis of lipoproteins by CHO($LpR_{1-790}LDLR_{791-839}$), *ldlA*($LpR_{1-342}LDLR_{293-839}$) and *ldlA*($LDLR_{1-292}LpR_{343-850}$)

To test the transfectants for functional expression of hybrid receptors, the cells were incubated for 15 minutes at 37°C in

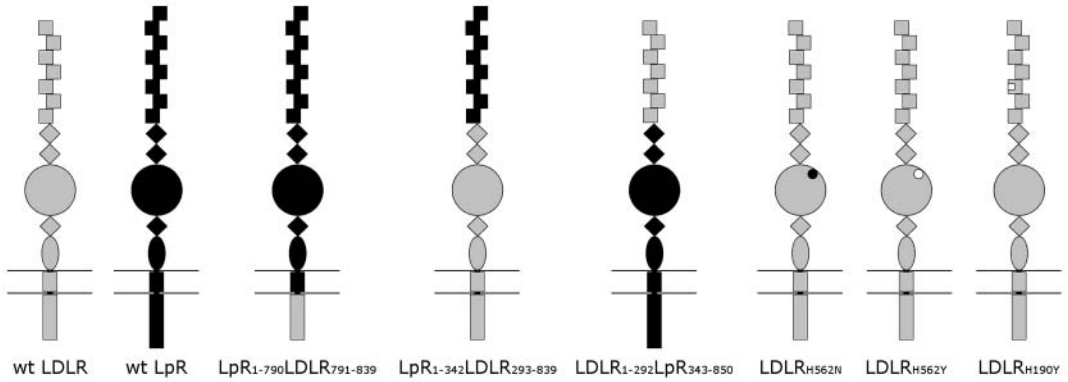

Fig. 2. Schematic models of wt LDLR, wt LpR, $LpR_{1-790}LDLR_{791-839}$, $LpR_{1-342}LDLR_{293-839}$, $LDLR_{1-292}LpR_{343-850}$, $LDLR_{H562N}$, $LDLR_{H562Y}$ and $LDLR_{H190Y}$; LDLR domains are depicted in grey and LpR domains in black. $LpR_{1-790}LDLR_{791-839}$ is composed of the ectodomain and transmembrane domain of LpR, and the intracellular tail of LDLR. $LpR_{1-342}LDLR_{293-839}$ harbours the ligand-binding domain of LpR and the region from the EGF domain to the C-terminus of LDLR. $LDLR_{1-292}LpR_{343-850}$ is composed of the ligand-binding domain of LDLR and the region from the EGF domain to the C-terminus of LpR. In the mutant LDLR receptors, His562 is substituted by Tyr (small white circle in the β-propeller) or Asn (small black circle in the β-propeller), or His190 is mutated to Tyr (small white square in the fifth cysteine-rich repeat). Squares, ligand-binding domain; diamonds, EGF repeats; circle, β-propeller; oval, *O*-linked glycosylation domain; short rectangle, transmembrane domain; long rectangle, intracellular tail.

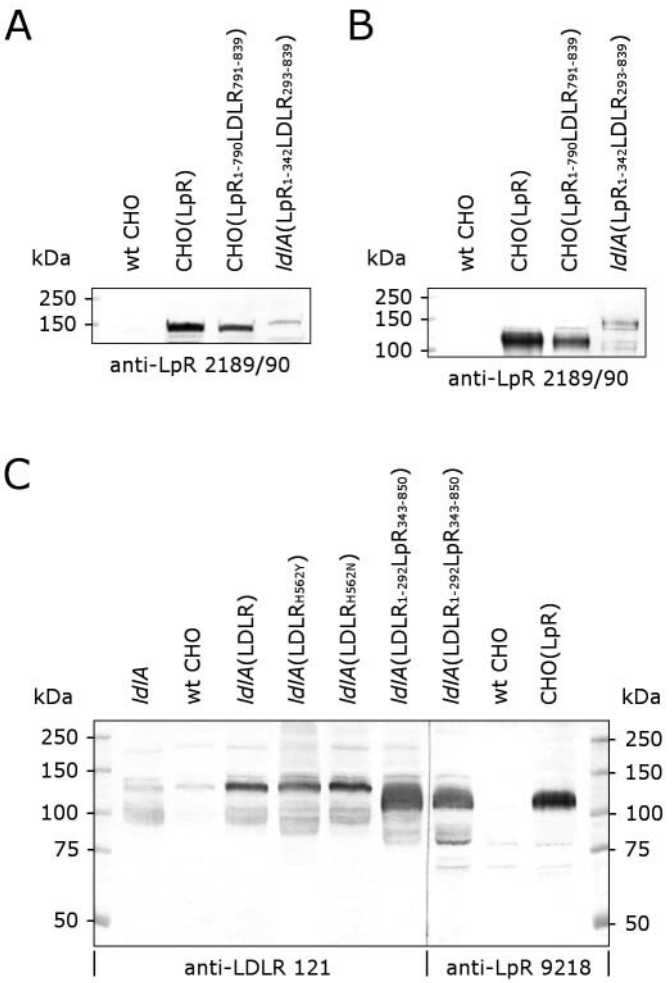

Fig. 3. (A,B) Western-blot analysis of membrane proteins isolated from wt CHO, CHO(LpR), CHO($LpR_{1\text{-}790}LDLR_{791\text{-}839}$) and *ldlA*($LpR_{1\text{-}342}LDLR_{293\text{-}839}$) cells (lanes 1-4, respectively). The samples were subjected to SDS-PAGE under reducing (A) or non-reducing (B) conditions and blotted onto PVDF membrane. The wt LpR, $LpR_{1\text{-}790}LDLR_{791\text{-}839}$ and $LpR_{1\text{-}342}LDLR_{293\text{-}839}$ were detected with anti-LpR antibody 2189/90. (C) Membrane proteins of LDLR-deficient *ldlA* (lane 1), wt CHO (lanes 2 and 8), *ldlA*(LDLR) (lane 3), *ldlA*($LDLR_{H562Y}$) (lane 4), *ldlA*($LDLR_{H562N}$) (lane 5), *ldlA*($LDLR_{1\text{-}292}LpR_{343\text{-}850}$) (lanes 6, 7) and CHO(LpR) cells (lane 9) were subjected to SDS-PAGE under non-reducing conditions and blotted onto PVDF membrane Lanes 1-6 were incubated with anti-LDLR antibody 121 and lanes 7-9 with anti-LpR antibody 9218. The size markers (in kDa) are indicated on the left (A-C) and right (C) of the blots.

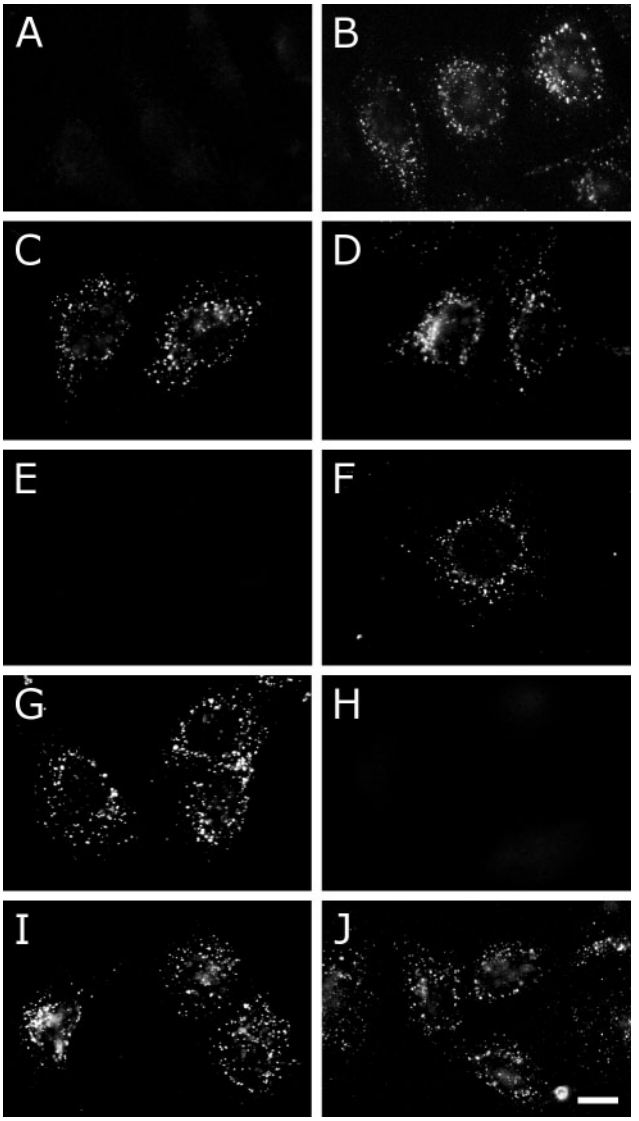

Fig. 4. Fluorescence-microscopic visualization of receptor-mediated endocytic uptake of fluorescently-labelled lipoprotein. Wild-type CHO (A), CHO(LpR) (B), CHO($LpR_{1\text{-}790}LDLR_{791\text{-}839}$) (C), *ldlA*($LpR_{1\text{-}342}LDLR_{293\text{-}839}$) (D) and *ldlA*($LDLR_{1\text{-}292}LpR_{343\text{-}850}$) (E) cells were incubated with OG-Lp in incubation medium for 15 minutes at 37°C, fixed and analysed with fluorescence microscopy. Similarly, *ldlA*(LDLR) (F), *ldlA*($LDLR_{1\text{-}292}LpR_{343\text{-}850}$) (G), *ldlA*($LpR_{1\text{-}342}LDLR_{293\text{-}839}$) (H), *ldlA*($LDLR_{H562N}$) (I) and *ldlA*($LDLR_{H562Y}$) cells (J) were incubated with OG-LDL. The grey dots (B-D,F,G,I,J) represent endocytic vesicles containing fluorescently labelled lipoprotein. Scale bar, 10 μm (J).

buffer supplemented with HEPES (i.e. incubation medium), containing OG-labelled lipoprotein. Lp specifically binds to LpR (Van Hoof et al., 2002; Van Hoof et al., 2003; Van Hoof et al., 2005) and is assumed to attach to the ligand-binding domain. Non-transfected cells are unable to endocytose the ligand and remain devoid of vesicles containing OG-labelled Lp (OG-Lp) upon incubation with the ligand (Fig. 4A). In CHO(LpR) cells, OG-Lp accumulates in endosomes that can be visualized with fluorescence microscopy (Fig. 4B) (Van Hoof et al., 2002). After OG-Lp incubation, a vesicle staining pattern identical to that of LpR-expressing transfectants was observed in CHO($LpR_{1\text{-}790}LDLR_{791\text{-}839}$) cells (Fig. 4C) as well as *ldlA*($LpR_{1\text{-}342}LDLR_{293\text{-}839}$) cells (Fig. 4D), but not in *ldlA*($LDLR_{1\text{-}292}LpR_{343\text{-}850}$) cells (Fig. 4E). These data suggest that $LpR_{1\text{-}790}LDLR_{791\text{-}839}$ and $LpR_{1\text{-}342}LDLR_{293\text{-}839}$ are functionally expressed. In addition, the finding that Lp is efficiently internalized by $LpR_{1\text{-}342}LDLR_{293\text{-}839}$, whereas $LDLR_{1\text{-}292}LpR_{343\text{-}850}$ lacks the ability to mediate endocytosis of the ligand, confirms that Lp docks onto the ligand-binding domain of LpR.

LDL was labelled with OG (OG-LDL) for incubation experiments similar to those described above. In contrast to

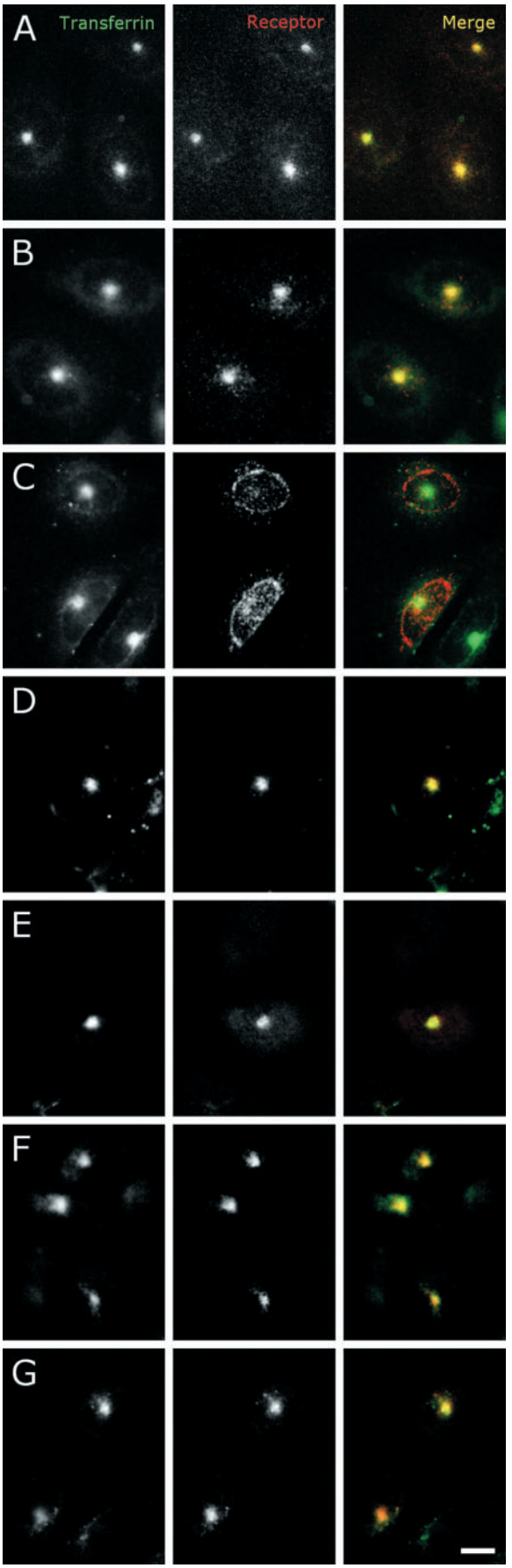

untransfected *ldlA* cells (data not shown), *ldlA*(LDLR) cells show a punctate fluorescence pattern upon incubation with OG-LDL (Fig. 4F), which is indicative of LDLR-mediated LDL endocytosis. Whereas *ldlA*($LDLR_{1-292}LpR_{343-850}$) transfectants show a similar staining pattern (Fig. 4G), *ldlA*($LpR_{1-342}LDLR_{293-839}$) are unable to internalize LDL (Fig. 4H). These observations suggest that, in addition to the other two hybrid receptors, $LDLR_{1-292}LpR_{343-850}$ is functionally expressed. Moreover, the ability of $LDLR_{1-292}LpR_{343-850}$ to internalize LDL, whereas $LpR_{1-342}LDLR_{293-839}$ does not mediate LDL uptake, implies that the LDLR EGF domain plays a trivial role in LDL binding.

Intracellular receptor distribution in the absence of lipoprotein

LpR was observed to recycle continuously in CHO cells without prior ligand binding (Van Hoof et al., 2002). Human Tf, a ligand that efficiently recycles via the ERC upon TfR-mediated endocytosis (Yamashiro et al., 1984; McGraw et al., 1987), colocalizes with wt LpR to the ERC (Van Hoof et al., 2002). After incubation of CHO(LpR) transfectants with OG-labelled Tf (OG-Tf) for 15 minutes at 37°C, followed by a 10-minute chase in growth medium without ligand, OG-Tf colocalizes with LpR that has converged in the ERC (Fig. 5A). In contrast to $LpR_{1-790}LDLR_{791-839}$, which also colocalizes with Tf (Fig. 5B), $LpR_{1-342}LDLR_{293-839}$ neither converged in a juxtanuclear organelle nor colocalized with Tf (Fig. 5C). These findings suggest that $LpR_{1-342}LDLR_{293-839}$ does not recycle constitutively.

Anti-LDLR antibody 121 recognizes non-functional intracellular LDLR intermediates expressed by *ldlA* cells under native, non-reducing conditions (Fig. 3C, lane 1) (Van Hoof et al., 2002). By contrast, anti-LDLR antibody C7 specifically binds to the properly folded first cysteine-rich repeat of the LDLR ligand-binding domain (Anderson et al., 1982) and allows exclusive visualization of the mature receptors. Similar to LpR, LDLR continuously recycles in the absence of lipoprotein (Goldstein et al., 1979) and is prominently present in the ERC (Fig. 5D). Under similar conditions, $LDLR_{1-292}LpR_{343-850}$ converged in the ERC as confirmed by colocalization with Tf (Fig. 5E), suggesting that this receptor also recycles constitutively.

Intracellular lipoprotein distribution after receptor-mediated endocytosis

CHO(LpR) transfectants resecrete Lp after LpR-mediated

Fig. 5. Colocalization of lipoprotein receptors with Tf in the ERC. Incubation of CHO(LpR) (A), CHO($LpR_{1-790}LDLR_{791-839}$) (B), *ldlA*($LpR_{1-342}LDLR_{293-839}$) (C), *ldlA*(LDLR) (D), *ldlA*($LDLR_{1-292}LpR_{343-850}$) (E), *ldlA*($LDLR_{H562N}$) (F) and *ldlA*($LDLR_{H562Y}$) transfectants (G) for 15 minutes with OG-Tf followed by a short chase of 10 minutes in growth medium shows that Tf accumulates in the ERC (left, grey). IF using anti-LpR antibody 2189/90 (A-C) or anti-LDLR antibody C7 (D-G) reveals that all receptors (middle, grey), except $LpR_{1-342}LDLR_{293-839}$ (C), also converge in this organelle and colocalize with Tf (right – Tf, green; receptor, red; colocalization, yellow). Scale bar, 10 μm (G, right).

endocytosis (Van Hoof et al., 2002). A 15-minute pulse with OG-Lp followed by a 60-minute chase at 37°C in growth medium without lipoprotein resulted in the disappearance of Lp, whereas LpR remains visible in the ERC (Fig. 6A). Similarly, CHO($LpR_{1-790}LDLR_{791-839}$) cells became depleted of vesicles containing OG-Lp after the chase and the hybrid receptor was predominantly found in the ERC in most of the cells (Fig. 6B). This suggests that, by analogy to LpR-mediated Lp recycling (Van Hoof et al., 2002), Lp is transported to the ERC after endocytic uptake by $LpR_{1-790}LDLR_{791-839}$ and is eventually resecreted from the cell. Thus, replacement of the intracellular tail of LpR by that of LDLR does not alter the ligand-recycling ability of LpR and suggests that this domain does not harbour unique motifs that are essential for ligand recycling.

Although a reduction of Lp was observed in *ldlA*($LpR_{1-342}LDLR_{293-839}$) cells, a significant amount of ligand remained in intracellular vesicles, and the ERC was devoid of hybrid receptor in most cells (Fig. 6C). This indicates that the ligand is not efficiently recycled and that the inability of $LpR_{1-342}LDLR_{293-839}$ to converge in the ERC remains unaffected after Lp endocytosis.

A similar pulse-chase experiment using *ldlA*(LDLR) cells incubated with OG-LDL results in a different ligand distribution. After the chase, LDL remains visible in vesicles that are scattered throughout the cell interior, whereas the receptor is predominantly localized to the ERC and does not colocalize with LDL (Fig. 6D). This indicates that, during the chase, the ligand is delivered to lysosomes, whereas the receptor continues to recycle. Under identical conditions, a similar dispersed LDL-containing vesicle pattern was visible in *ldlA*($LDLR_{1-292}LpR_{343-850}$) cells (Fig. 6E). However, the amount of receptor that had converged in the ERC had decreased (Fig. 6E). These results suggest that, in contrast to the intracellular distribution of both Lp-binding hybrid receptors, which is not altered upon Lp incubation, the transit of $LDLR_{1-292}LpR_{343-850}$ to the ERC is affected after LDL endocytosis. Taken together, our findings imply that the ligand-binding domain and the EGF domain of LpR are both involved in the process of LpR-driven ligand recycling; substitution of either domain by that of LDLR affects the recycling properties of the receptor.

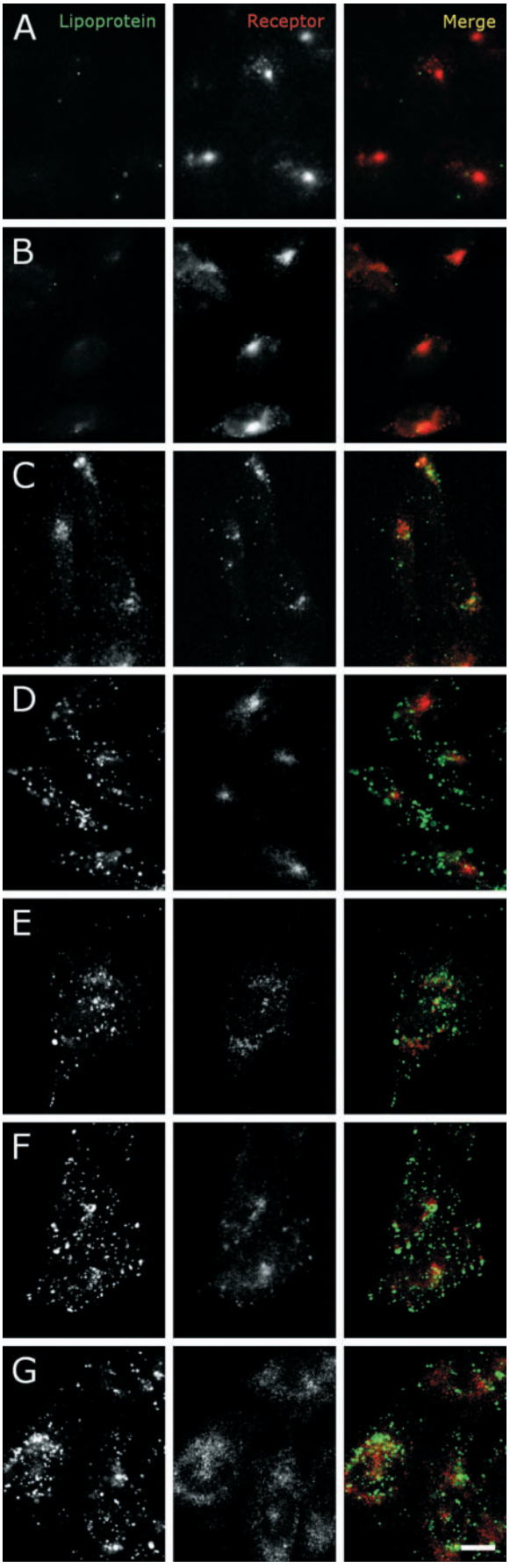

Fig. 6. Visualization of lipoprotein distribution after receptor-mediated endocytosis. CHO(LpR) (A), CHO($LpR_{1-790}LDLR_{791-839}$) (B), *ldlA*($LpR_{1-342}LDLR_{293-839}$) (C), *ldlA*(LDLR) (D), *ldlA*($LDLR_{1-292}LpR_{343-850}$) (E), *ldlA*($LDLR_{H562N}$) (F) and *ldlA*($LDLR_{H562Y}$) transfectants (G) were preincubated for 15 minutes with OG-Lp (A-C) or OG-LDL (D-G), followed by a 60-minute chase in growth medium without ligand. After fixation, the receptors were detected with IF using anti-LpR antibody 2189/90 (A-C) or anti-LDLR antibody C7 (D-G). Fluorescence microscopy reveals that CHO(LpR) (A) and CHO($LpR_{1-790}LDLR_{791-839}$) (B) transfectants have become depleted of lipoprotein (left), whereas the ligand remains visible in the other cell lines (C-G, grey). In contrast to wt LpR (A), $LpR_{1-790}LDLR_{791-839}$ (B) and wt LDLR (D), the other receptors are scattered throughout the cell and do not prominently converge in the ERC (middle, grey). Although they are more diffuse, the intracellular distributions of $LpR_{1-342}LDLR_{293-839}$ (C), $LDLR_{1-292}LpR_{343-850}$ (E), $LDLR_{H562N}$ (F) and $LDLR_{H562Y}$ (G) coincide with that of the internalized ligand (right – lipoprotein, green; receptor, red; colocalization, yellow). Scale bar, 10 μm (G, right).

In vitro analysis of $LDLR_{H562N}$ and the FH class-5 mutant $LDLR_{H562Y}$

To analyse the properties of $LDLR_{H562N}$ and $LDLR_{H562Y}$ (Fig. 2) at the cellular level, *ldlA* cells were transfected with the pcDNA3 vectors harbouring the mutagenized LDLR constructs, generating the cell lines *ldlA*($LDLR_{H562N}$) and *ldlA*($LDLR_{H562Y}$), respectively. Western-blot analysis using anti-LDLR antibody 121 shows that, under non-reducing conditions, $LDLR_{H562N}$ and $LDLR_{H562Y}$ have an electrophoretic mobility identical to wt human LDLR (Fig. 3C), suggesting that these receptors are folded correctly. Endocytic uptake of OG-LDL by *ldlA*($LDLR_{H562N}$) (Fig. 4I) and *ldlA*($LDLR_{H562Y}$) cells (Fig. 4J) indicates that both receptors are functionally expressed. Moreover, in the absence of LDL, the receptors colocalize with OG-Tf to the ERC (Fig. 5F,G), suggesting that $LDLR_{H562N}$ and $LDLR_{H562Y}$ are able to recycle constitutively. By contrast, a pulse-chase experiment with OG-LDL alters the recycling pathway of $LDLR_{H562N}$ and $LDLR_{H562Y}$, similar to $LDLR_{1\text{-}292}LpR_{343\text{-}850}$ (Fig. 6E). As in *ldlA*(LDLR) cells (Fig. 6D), LDL was retained in *ldlA*($LDLR_{H562N}$) and *ldlA*($LDLR_{H562Y}$) cells, but convergence of the mutagenized receptors in the ERC had decreased (Fig. 6F,G). These results indicate that mutation of His562 to Asn does not convert the ligand dissociation property of LDLR to LpR-like ligand recycling. Moreover, recent findings imply that substitution of the LDLR His562 residue significantly reduces the ability of these mutants to dissociate bound LDL at low pH (Beglova et al., 2004). Our findings coincide with these observations and suggest that replacement of the region from EGF domain to intracellular tail by that of LpR (i.e. $LDLR_{1\text{-}292}LpR_{343\text{-}850}$) similarly affects receptor recycling after LDL endocytosis.

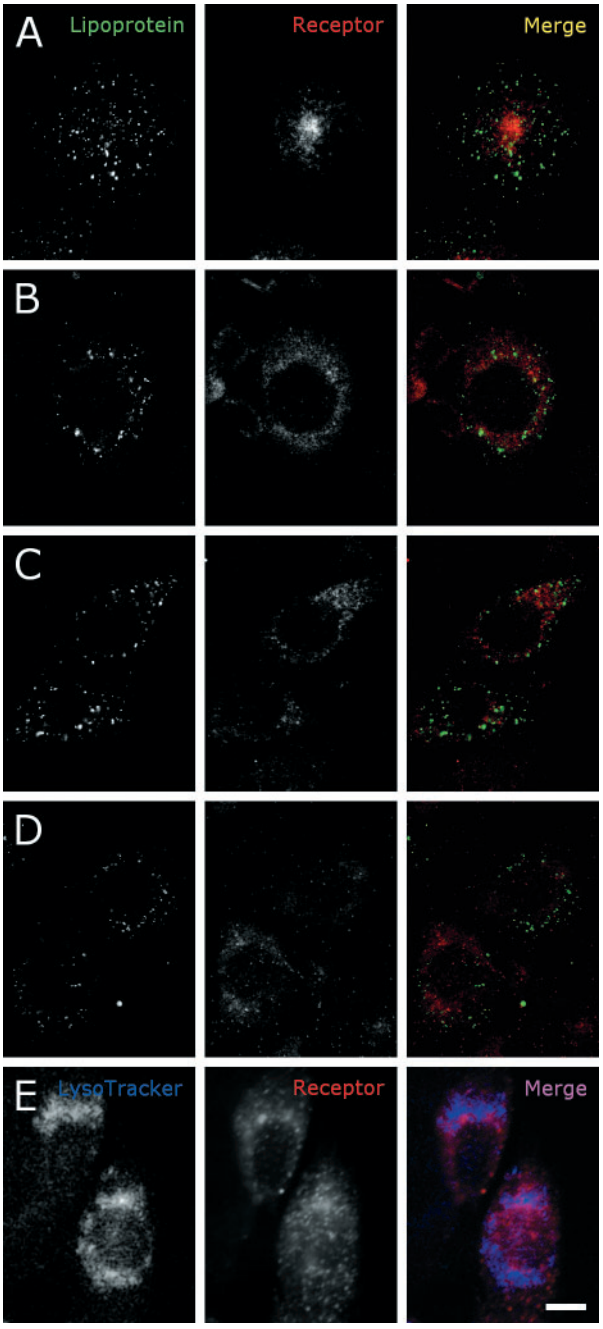

Reduction of RRE upon prolonged LDL incubation

Whereas mutation of His562 to Tyr is presumed to result in impaired LDLR recycling in vivo (Sun et al., 1994) (J. C. Defesche, personal communication), the in vitro experiments described above show that this $LDLR_{H562Y}$ mutant as well as $LDLR_{H562N}$ and $LDLR_{1\text{-}292}LpR_{343\text{-}850}$ is prominently present in the ERC in the absence of LDL. To mimic in vivo conditions in which LDL is constantly present, transfectants were preincubated for 90 minutes in growth medium with unlabelled LDL before a pulse of 15 minutes with OG-LDL. Endocytic uptake of OG-LDL by wt LDLR was not perceptibly reduced and the receptor was eminently concentrated in the ERC (Fig. 7A). Thus, continuous LDL endocytosis affects neither recycling of LDLR nor LDLR-mediated LDL uptake. By contrast, a significant decrease was observed in LDL endocytosis by *ldlA*($LDLR_{1\text{-}292}LpR_{343\text{-}850}$), *ldlA*($LDLR_{H562N}$) and *ldlA*($LDLR_{H562Y}$), and the ERC was almost devoid of receptor (Fig. 7B-D). Instead of converging in the ERC, the receptor distribution was dispersed and less intense, suggesting transit of these receptors to lysosomes. This notion is supported by the distribution pattern of a lysosomal marker coinciding

Fig. 7. Visualization of LDL uptake and receptor distribution when LDL is continuously present. In contrast to *ldlA*(LDLR), LDL uptake by *ldlA*($LDLR_{H562Y}$), *ldlA*($LDLR_{H562N}$) and *ldlA*($LDLR_{1\text{-}292}LpR_{343\text{-}850}$) transfectants is reduced and receptors are not prominently localized to the ERC after prolonged LDL incubation. Transfectants were preincubated for 90 minutes in growth medium with unlabelled LDL, followed by a 15-minute pulse with OG-LDL; the receptor was stained for IF using anti-LDLR antibody C7. Whereas OG-LDL uptake by wt LDLR (A) is not visibly affected upon LDL preincubation, and ligand (left, grey) and receptor (middle, grey) do not colocalize (right – ligand, green; receptor, red; colocalization, yellow), OG-LDL endocytosis by *ldlA*($LDLR_{1\text{-}292}LpR_{343\text{-}850}$) (B), *ldlA*($LDLR_{H562N}$) (C) and *ldlA*($LDLR_{H562Y}$) transfectants (D) is decreased, and the receptors are not prominently concentrated in the ERC. (E) $LDLR_{H562Y}$ appears scattered throughout the cell interior after a 105-minute incubation with unlabelled LDL, reducing receptor visibility to some extent (middle, grey). The receptor distribution is similar to that of the lysosomal marker (left, grey; right – LysoTracker, blue; receptor, red; colocalization, magenta). Scale bar, 10 μm (E, right).

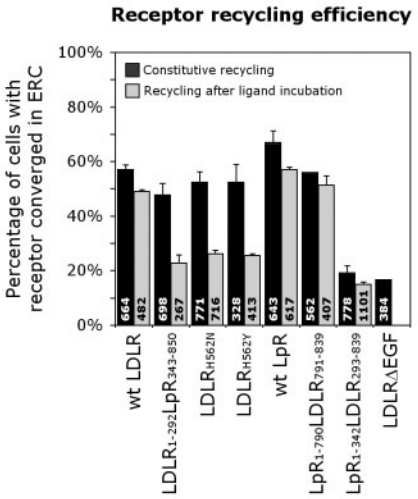

Fig. 8. Quantification of constitutive RRE (black) by counting the relative numbers of transfectants in which the receptor had perceptibly converged in the ERC after a short pulse of fluorescently labelled ligand. RRE after prolonged lipoprotein incubation (grey) was determined after a similar pulse preceded by a 90-minute preincubation of unlabelled ligand. *ldlA*(LDLR), *ldlA*($LDLR_{1\text{-}292}LpR_{343\text{-}850}$), *ldlA*($LDLR_{H562N}$) and *ldlA*($LDLR_{H562Y}$) transfectants were incubated with LDL, and CHO(LpR), CHO($LpR_{1\text{-}790}LDLR_{791\text{-}839}$) and *ldlA*($LpR_{1\text{-}342}LDLR_{293\text{-}839}$) transfectants with Lp. Error bars show s.d. of each duplicate experiment (s.d. $LpR_{1\text{-}790}LDLR_{791\text{-}839} < 0.1\%$; LDLRΔEGF, single experiment). The total number of cells counted for each data set is indicated at the bottom of each bar.

with $LDLR_{H562Y}$ (Fig. 7E) and the other LDLR variants (data not shown).

Quantification of RRE

To quantify constitutive RRE, the relative number of transfectants in which the receptors perceptibly converged in the ERC was determined after a short pulse with OG-labelled LDL or Lp. IF analysis revealed that in ~57% of *ldlA*(LDLR) transfectants that had internalized OG-LDL during a 15-minute pulse, wt LDLR was prominently localized in the ERC (Fig. 8). The HEPES component of incubation medium inhibits acidification of the endosome lumen (Sullivan et al., 1987), thus preventing LDL release after receptor-mediated endocytosis and subsequent transition of LDLR to the ERC. Under these conditions, ERC-located LDLR represents the pool of receptors that were internalized before LDL incubation and in the process of recycling. Therefore, the proportion of cells in which LDLR was discernibly situated in the ERC is an indication for constitutive RRE of wt human LDLR in CHO cells. Under identical conditions, the constitutive RREs of $LDLR_{1\text{-}292}LpR_{343\text{-}850}$ (48%), $LDLR_{H562N}$ (52%) and $LDLR_{H562Y}$ (52%) closely matched that of wt LDLR (Fig. 8), suggesting that these receptors are not affected in their ability to recycle constantly.

CHO(LpR), CHO($LpR_{1\text{-}790}LDLR_{791\text{-}839}$) and *ldlA*($LpR_{1\text{-}342}LDLR_{293\text{-}839}$) transfectants were analysed using OG-Lp, showing that the constitutive RREs of wt *L. migratoria* LpR (67%) and $LpR_{1\text{-}790}LDLR_{791\text{-}839}$ (56%) are approximately similar to that of the LDL-binding receptors (Fig. 8). By contrast,

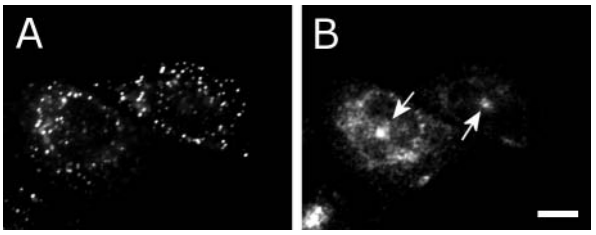

Fig. 9. $LDLR_{H190Y}$ can recycle constitutively and mediates endocytic uptake of LDL in vitro. The *ldlA*($LDLR_{H190Y}$) transfectants were incubated with OG-LDL for 15 minutes (A), after which the receptor was visualized with anti-LDLR antibody C7 (B) following fixation. The arrows indicate the ERC in transfected cells (B). Scale bar, 10 μm (B).

the RRE of $LpR_{1\text{-}342}LDLR_{293\text{-}839}$ is three times lower (20%) than that of the other Lp-binding receptors (Fig. 8), which coincides with the microscopic visualization analysis (Fig. 5C). Concurrently, the constitutive RRE of an LDLR deletion mutant whose complete EGF domain was removed (LDLRΔEGF) (Davis et al., 1987) is ~17% (Fig. 8). This indicates that, like $LpR_{1\text{-}342}LDLR_{293\text{-}839}$, LDLRΔEGF is not efficiently recycled via the ERC, which is consistent with its presumed fate in vitro (Davis et al., 1987) (J. L. Goldstein, personal communication) as well as in vivo (Miyake et al., 1989).

Apparently, recycling of ligand-free receptors is impaired neither when the LDLR region from the EGF domain to the C-terminus is replaced by that of LpR (i.e. $LDLR_{1\text{-}292}LpR_{343\text{-}850}$) nor when His562 of LDLR is substituted with Tyr or Asn. However, a decrease in ERC convergence of these receptors upon prolonged LDL incubation (Fig. 7B-D) suggests that the internalization of ligand inhibits receptor recycling via the ERC. The effect of prolonged LDL incubation on the RRE of the LDL-binding mutants was quantified after a 90-minute prepulse with normal growth medium containing unlabelled LDL followed by a 15-minute pulse with OG-LDL. Whereas, under these conditions, the RRE of wt LDLR (49%) decreased by less than 10%, those of $LDLR_{1\text{-}292}LpR_{343\text{-}850}$ (23%), $LDLR_{H562N}$ (26%) and $LDLR_{H562Y}$ (26%) halved, approaching the constitutive RREs of $LpR_{1\text{-}342}LDLR_{293\text{-}839}$ and LDLRΔEGF (Fig. 8). These findings support the microscopic data (Fig. 7B-D) and suggest that recycling of these receptors is impaired upon LDL endocytosis. Prolonged incubation of CHO(LpR), CHO($LpR_{1\text{-}790}LDLR_{791\text{-}839}$) and *ldlA*($LpR_{1\text{-}342}LDLR_{293\text{-}839}$) cells with Lp slightly decreased the RRE of the Lp-binding receptors (Fig. 8), which is similar to that found for wt LDLR. The minor reduction indicates that the RRE is not significantly affected by endocytosis of Lp.

In vitro analysis of the FH class-5 mutant $LDLR_{H190Y}$

Not only His562 but also His190 and His586 of the pH-sensitive triad of LDLR are proposed to participate in stabilizing the folded conformation of LDLR at endosomal pH (Rudenko et al., 2002). Although no His586 mutation has been reported to be associated with FH, mutation of His190 to Tyr is clinically diagnosed as FH and suggested to inhibit the transition of the receptor from endoplasmic reticulum to the Golgi apparatus and consequently to the cell surface (Hopkins et al., 1999) [i.e. class 2 (Hobbs et al., 1992)]. In vitro data

show that expression of $LDLR_{H190Y}$ (Fig. 2) by stably transfected *ldlA* cells enables these cells to endocytose LDL (Fig. 9A), suggesting that this mutation prevents neither proper cell-surface expression of the receptor nor LDL binding and subsequent receptor-mediated endocytosis, and hence does not belong to class 2, 3 or 4 (Hobbs et al., 1992). IF analysis reveals that the receptor prominently converges in the ERC (Fig. 9B), indicating that $LDLR_{H190Y}$ is able to recycle constitutively. It was recently shown that $LDLR_{H190Y}$ is expressed at normal levels and is only mildly affected in its ability to release bound LDL at a low pH (Beglova et al., 2004). Although it remains to be investigated whether $LDLR_{H190Y}$ shows reduced RRE upon prolonged LDL incubation, these combined findings suggest that this FH mutation either belongs to class-5 mutations that impair receptor recycling after ligand endocytosis or is a receptor polymorphism.

Discussion

Recently, several insect LDLR family members have been identified that bind the insect lipoprotein Lp (Dantuma et al., 1999; Cheon et al., 2001; Seo et al., 2003; Lee et al., 2003a; Lee et al., 2003b), the apolipoprotein matrix of which is structurally related to that in mammalian LDL (Babin et al., 1999; Mann et al., 1999; Segrest et al., 2001). *L. migratoria* LpR was the first insect LDLR homologue to be cloned (Dantuma et al., 1999) and characterized in vitro in mammalian (Van Hoof et al., 2002) and insect (Van Hoof et al., 2005) cells, as well as in *L. migratoria* fat body tissue (Van Hoof et al., 2003; Van Hoof et al., 2005), in which it mediates endocytic uptake of Lp. These studies additionally revealed that Lp is recycled upon LpR-mediated endocytosis (Van Hoof et al., 2002). Resecretion of apolipoproteins such as apoE has been described (Heeren et al., 1999), but Lp recycling is unique in several ways: (1) Lp is a native lipoprotein comprising an apolipoprotein matrix and a lipid moiety; (2) Lp remains attached to its receptor, in contrast to apoE (Farkas et al., 2004; Heeren et al., 2004); and (3) Lp recycles via the ERC, whereas apoE is resecreted from peripheral recycling endosomes (Heeren et al., 1999). Although resecretion of intact Lp contributes to the ability of Lp to function as a reusable lipid shuttle (Ryan and Van der Horst, 2000; Arrese et al., 2001; Van der Horst et al., 2001; Van der Horst et al., 2002), it is in conflict with the classic lysosomal pathway for mammalian lipoproteins like LDL and very-low-density lipoprotein (VLDL) (Goldstein et al., 1985; Brown and Goldstein, 1986; Tacken et al., 2001). We set out to identify the domains of LpR that determine the fate of a lipoprotein after endocytosis.

Multiple domains of LpR were exchanged with LDLR domains to generate hybrid lipoprotein receptors that contain all five typical domains (Fig. 2). Replacing the intracellular tail of LpR with that of LDLR ($LpR_{1\text{-}790}LDLR_{791\text{-}839}$) did not significantly affect the ligand recycling properties of the receptor (Fig. 5B, Fig. 6B). However, when substitution of the LpR domains was extended to the EGF domain, transit of the resulting hybrid receptor ($LpR_{1\text{-}342}LDLR_{293\text{-}839}$) through the ERC was inhibited (Fig. 5C) and receptor-mediated ligand recycling was impaired (Fig. 6C). These findings suggest that recycling of LpR and its ligand is not solely determined by the cytosolic tail of LpR but involves the ectodomain. Notably, the intracellular fate of $LpR_{1\text{-}342}LDLR_{293\text{-}839}$ resembles that of a mutant LDLR, the EGF domain of which was deleted (i.e. LDLRΔEGF) (Davis et al., 1987). In vitro analysis showed that the affinity of LDLRΔEGF for LDL is dramatically reduced (Davis et al., 1987) although it retains the ability to bind LDL on ligand blots (S. C. Blacklow, personal communication). Whereas the ability of the mutant receptor to bind VLDL is maintained, ligand (i.e. VLDL) uncoupling is impaired (Davis et al., 1987). As a result, the receptor-ligand complex is degraded in lysosomes; its fate in vivo is assumed to be identical (Miyake et al., 1989). The affinity of $LpR_{1\text{-}342}LDLR_{293\text{-}839}$ for Lp was not visibly affected. Yet recycling of the receptor was inhibited, which is a characteristic of FH class-5 LDLR mutants (Hobbs et al., 1992) like LDLRΔEGF.

In contrast to $LpR_{1\text{-}342}LDLR_{293\text{-}839}$, the reciprocal hybrid composed of the ligand-binding domain of LDLR and the other domains of LpR ($LDLR_{1\text{-}292}LpR_{343\text{-}850}$) converged in the ERC in the absence of ligand (Fig. 5E). Apparently, the ligand-binding domain of LpR is not essential for recycling of ligand-free receptors. By contrast, ligand endocytosis significantly reduced the RRE of this receptor (Fig. 7B, Fig. 8). Together, the findings with $LpR_{1\text{-}342}LDLR_{293\text{-}839}$ and $LDLR_{1\text{-}292}LpR_{343\text{-}850}$ suggest both that the ligand-binding domain and EGF domain are involved in LpR-driven ligand recycling and that these domains cooperate during this process.

The ligand-binding domain and the EGF domain of LDLR have been shown to interact at endosomal pH. The X-ray crystal structure of the LDLR ectodomain reveals that, at low pH, the ligand-binding domain is folded onto the β-propeller of the EGF domain (Rudenko et al., 2002), which thereby occupies the binding site for LDL (Innerarity, 2002; Jeon and Blacklow, 2003). Thus, the EGF domain is presumed to function as an alternative ligand that displaces LDL from the ligand-binding domain upon acidification of the sorting-endosome lumen (Innerarity, 2002; Jeon and Blacklow, 2003). Ligand uncoupling is essential for LDLR recycling (Davis et al., 1987; Hobbs et al., 1992) but it is not a prerequisite for LpR to be transferred to the ERC (Van Hoof et al., 2002). Even though wt LpR harbours an EGF domain, bound ligand remains attached and is recycled in complex with LpR. This suggests that the EGF domain of LpR lacks a pH-sensitive switch that induces ligand uncoupling.

A triad of His residues that become protonated at pH below 6.7 has been found to participate in establishing the arched conformation of the LDLR ectodomain at endosomal pH (Rudenko et al., 2002). Two of these three residues, His562 and His586, are in the EGF domain. Superimposing the three-dimensional model of LpR onto the elucidated structure of the LDLR ectodomain at pH 5.3 (Rudenko et al., 2002) reveals that only two of the three His residues in LDLR are present in LpR: His562 corresponds to Asn643 in LpR of *L. migratoria* (Fig. 1) and other insects (D. Van Hoof and K. W. Rodenburg, unpublished). This suggests that wt LpR lacks an essential triadic His residue in the EGF domain, which in LDLR is presumed to participate in the process of ligand dissociation (Innerarity, 2002; Jeon and Blacklow, 2003; Beglova et al., 2004). The absence of this triadic His residue in LpR might explain the stability of the receptor-ligand complex in sorting endosomes, which is a prerequisite for LpR-mediated ligand recycling. It would seem plausible that the $LpR_{1\text{-}342}LDLR_{293\text{-}839}$ hybrid, harbouring the LDLR EGF domain, is able to dissociate Lp and recycle afterwards.

However, the fluorescence microscopic data suggest that the ligand remains attached to the receptor and that the receptor-ligand complex is not recycled (Fig. 6C, Fig. 8). This indicates that additional LDLR elements participating in ligand uncoupling are not present in LpR, and that these motifs are receptor-type specific.

To investigate whether LpR-analogous insensitivity for an acidic environment (i.e. maintenance of a receptor-ligand complex in sorting endosomes) could be introduced into LDLR, His562 was mutated to Asn ($LDLR_{H562N}$). The mutant receptor was observed to internalize LDL (Fig. 4I) and to recycle constitutively through the ERC (Fig. 5F), but internalized ligand was retained in the cell (Fig. 6F). These findings demonstrate that the receptor is functionally expressed and suggest that Asn562 in itself does not evoke ligand recycling. Whereas $LDLR_{H562N}$ recycles normally in the absence of ligand (Fig. 5F, Fig. 8), RRE was significantly reduced upon prolonged LDL incubation (Fig. 8). The observations that receptor recycling is only impaired after ligand internalization and that the ligand is retained in the cell suggest that His562 is essential for ligand uncoupling but not for constitutive receptor recycling. Identical results were obtained with $LDLR_{H562Y}$. A significant reduction in ligand uncoupling of bound LDL at low pH has recently been shown for $LDLR_{H562Y}$ using flow cytometry (Beglova et al., 2004). Thus, the FH class-5 mutation H562Y (Sun et al., 1994) (J. C. Defesche, personal communication) apparently impairs ligand dissociation and subsequent receptor recycling, whereas constitutive recycling of the receptor remains unaffected.

The third triadic His residue (i.e. His190) resides in the fifth cysteine-rich repeat of the ligand-binding domain of LDLR (Fig. 1). Mutation of His190 to Tyr was found to result in FH (Hopkins et al., 1999) and was postulated to be a class-2 mutation [affecting transit of the receptor from endoplasmic reticulum to Golgi complex (Hobbs et al., 1992)]. Although a mutation in the ligand-binding domain could belong to class 3 (i.e. binding deficient), our in vitro data show that $LDLR_{H190Y}$ is capable of LDL endocytosis (Fig. 9A) as well as constitutive recycling (Fig. 9B). These results exclude this receptor from class 2 and 3 as supported by Beglova et al. (Beglova et al., 2004) and class 4 (i.e. endocytosis deficient) (Hobbs et al., 1992), and imply that $LDLR_{H190Y}$ is impaired in uncoupling the ligand after endocytosis, resulting in degradation of the receptor-ligand complex (i.e. class 5) (Hobbs et al., 1992). The construction of additional hybrids of LDLR and LpR, an LpRΔEGF deletion mutant, and point mutations of amino acid residues located in the ligand-binding domain and EGF domain of LDLR and LpR (e.g. $LDLR_{H586Y}$ and LpR_{N643H}) will contribute to the understanding of ligand dissociation and subsequent recycling of lipoprotein receptors in general.

The present findings with hybrid receptors composed of LpR and LDLR domains reveal that lipoprotein recycling by LpR, which is unique for an LDLR homologue composed of all five domains, depends on the cooperation between its ligand-binding and EGF domains. Additionally, the LDLR mutants provided information about the role of the triadic His residues in ligand dissociation as well as receptor recycling. LDLR that fails to uncouple LDL owing to mutation or the absence of essential residues or domains is destined to be degraded in lysosomes (Davis et al., 1987). Although studies with the VLDL receptor (Mikhailenko et al., 1999) and LpR (Van Hoof et al., 2002) indicate that ligand dissociation is not a prerequisite for all lipoprotein receptors to recycle, it appears to be a crucial step for LDLR to maintain cholesterol homeostasis in vivo (Brown and Goldstein, 1986; Hobbs et al., 1992). The conformational change of LDLR (Rudenko et al., 2002), through which the ligand is displaced from the ligand-binding domain (Innerarity, 2002; Jeon and Blacklow, 2003), is probably essential in order to pass a quality check that discriminates between receptors in a ligand-free state and those in complex with ligand. If ligand remains bound to LDLR, the ligand-binding domain cannot fold properly onto the EGF domain (Rudenko et al., 2002; Jeon and Blacklow, 2003). Mutations in the EGF and ligand-binding domains could inhibit the formation or affect the stability of the folded conformation. In either case, the receptor does not comply the conditions required for recycling. As a consequence, transfer to the cell surface is prohibited; the receptor is directed to lysosomes (Fig. 7E) and degraded.

Whereas some mutations only prevent receptor recycling when ligand displacement is impaired (e.g. H562Y and possibly H190Y), others render LDLR incapable of adopting a conformational change in the presence as well as absence of ligand (e.g. LDLRΔEGF); both cases would increase receptor turnover in vivo. No LDLR mutations have yet been reported that inhibit LDL dissociation without preventing the receptor to recycle in complex with ligand, in a manner similar to LpR. Such mutations would, however, also lead to elevated plasma cholesterol levels in vivo, because there will be no net removal of circulating LDL particles.

Taken together, the present data provide insight into the domains and residues involved in LpR-specific ligand recycling and the recycling of LDLR family members in general. Moreover, the findings propound that FH class-5 LDLR mutations can be divided into two distinct subclasses: (1) those that retain constitutive receptor recycling but inhibit ligand dissociation, resulting in receptor-ligand complex degradation (e.g. $LDLR_{H562Y}$); and (2) those that completely impede recycling of the receptor in the absence as well as presence of ligand (e.g. LDLRΔEGF). LDLR FH mutations that impair ligand dissociation without preventing the receptor to recycle in complex with ligand in a manner similar to LpR would compose a third subclass. Such a phenotype might be rare because it probably requires more than one mutation, involving the EGF domain as well as the ligand-binding domain. In-vitro analysis using fluorescence microscopy to analyse FH mutations at the cellular level provides a powerful tool to classify mutations properly in clinically diagnosed FH patients.

We thank: J. L. Goldstein (University of Texas Southwestern Medical Center, Dallas, TX) for the TR715-19 [*ldlA*(LDLR)] and TR841a-2 [*ldlA*(LDLRΔEGF)] cell lines, and for stimulating discussions about intracellular LDLR pathways; S. C. Blacklow (Brigham and Women's Hospital and Harvard Medical School, Boston, MA) for details about the ligand-binding properties of LDLR and LDLR muntants; L. J. Braakman and J. Gent for anti-human-LDLR mouse antibody C7 and anti-human-LDLR rabbit antibody 121, and for the pBS-LDLR human *LDLR* cDNA clone; D. K. Strickland for information about ligand binding and recycling properties of VLDLRΔEGF; P. N. Hopkins and M. Emi for correspondence about the H190Y mutation; J. C. Defesche (Academic Medical Center at the University of Amsterdam, Amsterdam, The

Netherlands) for unpublished information about the Turkish $LDLR_{H562Y}$ mutation; S. D. Roosendaal (Utrecht University, Utrecht, The Netherlands) for unpublished details about the hybrid receptors and LDLR mutants; and J. Kerver for making the receptor constructs. This work was supported by the Earth and Life Sciences Foundation (ALW), which is subsidized by the Netherlands Organization for Scientific Research (NWO) (ALW-809.38.003).

References

Anderson, R. G. W., Brown, M. S., Beisigel, U. and Goldstein, J. L. (1982). Surface distribution and recycling of the low density lipoprotein receptor as visualized with antireceptor antibodies. *J. Cell Biol.* **93**, 523-531.

Arrese, E. L., Canavoso, L. E., Jouni, Z. E., Pennington, J. E., Tsuchida, K. and Wells, M. A. (2001). Lipid storage and mobilization in insects: current status and future directions. *Insect Biochem. Mol. Biol.* **31**, 7-17.

Babin, P. J., Bogerd, J., Kooiman, F. P., van Marrewijk, W. J. A. and van der Horst, D. J. (1999). Apolipophorin II/I, apolipoprotein B, vitellogenin, and microsomal triglyceride transfer protein genes are derived from a common ancestor. *J. Mol. Evol.* **49**, 150-160.

Beglova, N., Jeon, H., Fisher, C. and Blacklow, S. C. (2004). Cooperation between fixed and low pH-inducible interfaces controls lipoprotein release by the LDL receptor. *Mol. Cell* **16**, 281-292.

Brown, M. S. and Goldstein, J. L. (1986). A receptor-mediated pathway for cholesterol homeostasis. *Science* **232**, 34-47.

Cheon, H. M., Seo, S. J., Sun, J., Sappington, T. W. and Raikhel, A. S. (2001). Molecular characterization of the VLDL receptor homolog mediating binding of lipophorin in oocyte of the mosquito *Aedes aegypti*. *Insect Biochem. Mol. Biol.* **31**, 753-760.

Dantuma, N. P., Potters, M., de Winther, M. P., Tensen, C. P., Kooiman, F. P., Bogerd, J. and van der Horst, D. J. (1999). An insect homolog of the vertebrate very low density lipoprotein receptor mediates endocytosis of lipophorins. *J. Lipid Res.* **40**, 973-978.

Davis, C. G., Goldstein, J. L., Sudhof, T. C., Anderson, R. G., Russell, D. W. and Brown, M. S. (1987). Acid-dependent ligand dissociation and recycling of LDL receptor mediated by growth factor homology region. *Nature* **326**, 760-765.

Farkas, M. H., Weisgraber, K. H., Shepherd, V. L., Linton, M. F., Fazio, S. and Swift, L. L. (2004). The recycling of apolipoprotein E and its amino-terminal 22 kDa fragment: evidence for multiple redundant pathways. *J. Lipid Res.* **45**, 1546-1554.

Goldstein, J. L., Anderson, R. G. and Brown, M. S. (1979). Coated pits, coated vesicles, and receptor-mediated endocytosis. *Nature* **279**, 679-685.

Goldstein, J. L., Brown, M. S., Anderson, R. G. W., Russell, D. W. and Schneider, W. J. (1985). Receptor-mediated endocytosis: concepts emerging from the LDL receptor system. *Annu. Rev. Cell Biol.* **1**, 1-39.

Guex, N. and Peitsch, M. C. (1997). SWISS-MODEL and the Swiss-PdbViewer: an environment for comparative protein modelling. *Electrophoresis* **18**, 2714-2723.

Heeren, J., Weber, W. and Beisiegel, U. (1999). Intracellular processing of endocytosed triglyceride-rich lipoproteins comprises both recycling and degradation. *J. Cell Sci.* **112**, 349-359.

Heeren, J., Grewal, T., Laatsch, A., Becker, N., Rinninger, F., Rye, K. A. and Beisiegel, U. (2004). Impaired recycling of apolipoprotein E4 is associated with intracellular cholesterol accumulation. *J. Biol. Chem.* **279**, 55483-55492.

Hobbs, H. H., Brown, M. S. and Goldstein, J. L. (1992). Molecular genetics of the LDL receptor gene in familial hypercholesterolemia. *Hum. Mutat.* **1**, 445-466.

Hopkins, P. N., Wu, L. L., Stephenson, S. H., Xin, Y., Katsumata, H., Nobe, Y., Nakajima, T., Hirayama, T., Emi, M. and Williams, R. R. (1999). A novel LDLR mutation, H190Y, in a Utah kindred with familial hypercholesterolemia. *J. Hum. Genet.* **44**, 364-367.

Innerarity, T. L. (2002). Structural biology. LDL receptor's beta-propeller displaces LDL. *Science* **298**, 2337-2339.

Jansens, A., van Duijn, E. and Braakman, I. (2002). Coordinated nonvectorial folding in a newly synthesized multidomain protein. *Science* **298**, 2401-2403.

Jeon, H. and Blacklow, S. C. (2003). An intramolecular spin of the LDL receptor beta propeller. *Structure* **11**, 133-136.

Kingsley, D. M. and Krieger, M. (1984). Receptor-mediated endocytosis of low density lipoprotein: somatic cell mutants define multiple genes required for expression of surface-receptor activity. *Proc. Natl. Acad. Sci. USA* **81**, 5454-5458.

Lee, C. S., Han, J. H., Kim, B. S., Lee, S. M., Hwang, J. S., Kang, S. W., Lee, B. H. and Kim, H. R. (2003a). Wax moth, *Galleria mellonella*, high density lipophorin receptor: alternative splicing, tissue-specific expression, and developmental regulation. *Insect Biochem. Mol. Biol.* **33**, 761-771.

Lee, C. S., Han, J. H., Lee, S. M., Hwang, J. S., Kang, S. W., Lee, B. H. and Kim, H. R. (2003b). Wax moth, *Galleria mellonella* fat body receptor for high-density lipophorin (HDLp). *Arch. Insect Biochem. Physiol.* **54**, 14-24.

Mann, C. J., Anderson, T. A., Read, J., Chester, S. A., Harrison, G. B., Kochl, S., Ritchie, P. J., Bradbury, P., Hussain, F. S., Amey, J. et al. (1999). The structure of vitellogenin provides a molecular model for the assembly and secretion of atherogenic lipoproteins. *J. Mol. Biol.* **285**, 391-408.

Maxfield, F. R. and McGraw, T. E. (2004). Endocytic recycling *Nat. Rev. Mol. Cell Biol.* **5**, 121-132.

McGraw, T. E., Greenfield, L. and Maxfield, F. R. (1987). Functional expression of the human transferrin receptor cDNA in Chinese hamster ovary cells deficient in endogenous transferrin receptor. *J. Cell Biol.* **105**, 207-214.

Mikhailenko, I., Considine, W., Argraves, K. M., Loukinov, D., Hyman, B. T. and Strickland, D. K. (1999). Functional domains of the very low density lipoprotein receptor: molecular analysis of ligand binding and acid-dependent ligand dissociation mechanisms. *J. Cell Sci.* **112**, 3269-3281.

Miyake, Y., Tajima, S., Funahashi, T. and Yamamoto, A. (1989). Analysis of a recycling-impaired mutant of low density lipoprotein receptor in familial hypercholesterolemia. *J. Biol. Chem.* **264**, 16584-16590.

Mukherjee, S., Ghosh, R. N. and Maxfield, F. R. (1997). Endocytosis. *Physiol. Rev.* **77**, 759-803.

Rudenko, G., Henry, L., Henderson, K., Ichtchenko, K., Brown, M. S., Goldstein, J. L. and Deisenhofer, J. (2002). Structure of the LDL receptor extracellular domain at endosomal pH. *Science* **298**, 2353-2358.

Ryan, R. O. and van der Horst, D. J. (2000). Lipid transport biochemistry and its role in energy production. *Annu. Rev. Entomol.* **45**, 233-568.

Schwede, T., Kopp, J., Guex, N. and Peitsch, M. C. (2003). SWISS-MODEL: an automated protein homology-modeling server. *Nucleic Acids Res.* **31**, 3381-3385.

Segrest, J. P., Jones, M. K., de Loof, H. and Dashti, N. (2001). Structure of apolipoprotein B-100 in low density lipoproteins. *J. Lipid Res.* **42**, 1346-1367.

Seo, S. J., Cheon, H. M., Sun, J., Sappington, T. W. and Raikhel, A. S. (2003). Tissue- and stage-specific expression of two lipophorin receptor variants with seven and eight ligand-binding repeats in the adult mosquito. *J. Biol. Chem.* **278**, 41954-41962.

Stoorvogel, W., Strous, G. J., Geuze, H. J., Oorschot, V. and Schwartz, A. L. (1991). Late endosomes derive from early endosomes by maturation. *Cell* **65**, 417-427.

Sullivan, P. C., Ferris, A. L. and Storrie, B. (1987). Effects of temperature, pH elevators, and energy production inhibitors on horseradish peroxidase transport through endocytic vesicles. *J. Cell Physiol.* **131**, 58-63.

Sun, X. M., Patel, D. D., Webb, J. C., Knight, B. L., Fan, L. M., Cai, H. J. and Soutar, A. K. (1994). Familial hypercholesterolemia in China. Identification of mutations in the LDL-receptor gene that result in a receptor-negative phenotype. *Arterioscler. Thromb.* **14**, 85-94.

Tacken, P. J., Hofker, M. H., Havekes, L. M. and van Dijk, K. W. (2001). Living up to a name: the role of the VLDL receptor in lipid metabolism. *Curr. Opin. Lipidol.* **12**, 275-279.

Van der Horst, D. J., van Marrewijk, W. J. A. and Diederen, J. H. B. (2001). Adipokinetic hormones of insect: Release, signal transduction, and responses. *Int. Rev. Cytol.* **211**, 179-240.

Van der Horst, D. J., van Hoof, D., van Marrewijk, W. J. A. and Rodenburg, K. W. (2002). Alternative lipid mobilization: the insect shuttle system. *Mol. Cell. Biochem.* **136**, 217-226.

Van Hoof, D., Rodenburg, K. W. and van der Horst, D. J. (2002). Insect lipoprotein follows a transferrin-like recycling pathway that is mediated by the insect LDL receptor homologue. *J. Cell Sci.* **115**, 4001-4012.

Van Hoof, D., Rodenburg, K. W. and van der Horst, D. J. (2003). Lipophorin receptor-mediated lipoprotein endocytosis in insect fat body cells. *J. Lipid Res.* **44**, 1431-1440.

Van Hoof, D., Rodenburg, K. W. and van der Horst, D. J. (2005). Receptor-mediated endocytosis and intracellular trafficking of lipoproteins and transferrin in insect cells. *Insect Biochem. Mol. Biol.* **35**, 117-128.

Yamashiro, D. J., Tycko, B., Fluss, S. R. and Maxfield, F. R. (1984). Segregation of transferrin to a mildly acidic (pH 6.5) para-Golgi compartment in the recycling pathway. *Cell* **37**, 789-800.